Journal of Renewable Energy and Smart Systems Vol.1, No.1, 2024: 49-63

Renewable Energy and Smart Systems

journal homepage: https://sanad.iau.ir/journal/res

Experimental Investigation of the Magnetic Field Effect Using Fe_3O_4 Ferrofluid and the Study of the Ultrasonic Phenomenon in Solar Water Desalination Efficiency

Kimya Samadi [1], Hamid Reza Goshayeshi [1*], Vahid Nejati[1], Seyyed Reza Saleh [1], Issa Chaer [2]

[1] *Department of Mechanical Engineering, Mashhad Branch, Islamic Azad University, Mashhad, Iran*

[2] *The School of Built Environment and Architecture, London South Bank University, SE1 0AA, London, United Kingdom*

Article info

Keywords:
Solar desalination
Fe_3O_4 nanofluid
magnetic field
ultrasonic phenomenon
solenoid

Article history:
Received: 26 Apr 2024
Accepted: 10 Jul 2024

Abstract

The global scarcity of potable water remains a pressing human challenge, given that 97% of the Earth's water is saline. Therefore, solar desalination that uses cheap solar energy is the best way to prepare fresh water. This study employs a solar desalination apparatus featuring 28 steps, with dimensions of 30 mm in height, 110 mm in width, and 840 mm in length. The present work was conducted to improve and increase this device's efficiency and water output by examining magnetic field impact using Fe_3O_4 ferrofluid. Also, the ultrasonic phenomenon's effect to increase the device's efficiency is carried out. To increase the daily production rate of fresh water, the mentioned device has been tested and optimized in various configurations including 1) Simple configuration, 2) incorporating magnetic filing sheets, 3) utilizing two solenoids at different turns of 275 and 1000, 4) employing Fe_3O_4 nanofluid, 5) with Fe_3O_4 nanofluid and magnetic filing sheets, 6) with Fe_3O_4 nanofluid, solenoids at different turns of 275 and 1000, 7) involving the ultrasonic phenomenon, 8) utilizing Fe_3O_4 (Iron (III) Oxide) nanofluid, solenoids, and ultrasonic phenomenon, experimentally tested and optimized. After examining the results, it was found that mode 8, which includes the combined effect of Fe_3O_4 nanofluid, solenoid, and ultrasonic phenomenon, had the highest water production rate compared to the simple mode and it could be a cost-effective choice. The device's efficiency from 55.2% in mode 1 has reached 63.4%,72.9%,74.3%,80.2%,87.5% respectively in mode 2,3,5,6, 8 and the basin temperature has reached the highest value of 66.8°C at 2 PM in mode 8. According to the test results, it could be concluded that the use of sonicated water with Fe_3O_4 Ferrofluid under magnetic field effect has led to a significant increase in the device efficiency.

[*] Corresponding author.
E-mail address: goshayeshi1655@mshdiau.ac.ir

1. Introduction

In recent decades, the increase in population and per capita consumption has led to a significant rise in the utilization of water resources. Water has an important role in all living organism on earth [A1]. Many experts believe that existing sources of drinking water will be unable to meet the growing human needs [A2]. One of the methods for freshwater production is the utilization of solar energy, which takes place in devices called solar water desalination [A3]. As a crucial resource, the sun holds the potential to meet future electricity demands, especially considering the limited nature of fossil fuel resources and the industrialization efforts of numerous countries seeking energy. Conventional methods such as desalination, reverse osmosis, and Multi-Stage Flash (MSF) for producing fresh and pure water are energy-intensive and reliant on fossil fuels. However solar water desalination proves to be not only cost-effective and economical but also utilizes conventional fuels and preserves energy resources [A4]. Fortunately, Iran, located in the solar belt of the world, stands as one of the most acceptable countries for harnessing solar energy. Iran's annual solar energy is about three thousand times the country's annual energy consumption [A5]. Solar desalination exhibits cost-effectiveness in this context. Nevertheless, several factors can reduce the efficiency of solar desalination, including limited capacity, the need for relatively large space, the storage requirements during adverse weather conditions, and, most importantly, a reduction in efficiency due to water channel blockage resulting from impurity deposition. These factors raise questions about the cost-effectiveness of solar desalination. However, solar desalination offers various advantages, such as the production of pure water, independence from additional operational equipment, freedom from reliance on conventional energy sources [A6], feasibility of local construction and repair, low cost, and the potential to obtain drinking water. Water desalination process must have parameters such as low energy, high quality and efficiency, easily use and purity of energy used for water desalination. Therefore, according to mentioned parameters, distillation method could be a suitable method for water desalination [A7]. Sun-based stills are the most prudent method for preparing fresh water [A8]. Solar still is one of the major ways of delivering potable water from contaminated water [A9]. These devices, are used in distant and arid regions to convert salty water into fresh water [A10]. The basic role of distillation is simple and it is similar to the way of nature might rain [A11]. In recent years, there has been an increase in research efforts aimed at enhancing the performance of solar water desalination systems to optimize their economic feasibility Scientists have explored various approaches, including the utilization of magnetic field effects, the use of nano-fluids such as Fe_3O_4, and the application of sonication, to improve the efficiency of these devices. Magnetic fields have been studied in different water treatment applications for more than 50 years [A12]. It is discovered that as the intensity of magnetic induction increases, the water evaporation rate increases too [A13]. It could be proved that the impact of the magnetic field depends on the time, the magnetic position, and magnetic density [A14]. In a study, Goharkhah et al. investigated the impact of a non-uniform alternating magnetic field on the flow of magnetic fluid and heat transfer in a channel. The results showed a 6% increase in pressure drop at Re=2000 and a frequency of 5 Hz; however, this increase in pressure drop was not significant enough to correspond to a noticeable enhancement in heat transfer [A15]. In another study conducted by Asad Rahman et al., research was carried out on the expansion of solar water desalination through the integration of a magnetic unit and a double-layer glass cover with water. They presented a physical model and experimental method to examine the results. The presence of a magnetic field was emphasized as a contributing factor to enhancing the efficiency of solar water desalination and the maximum of temperature in the basin water of solar still was 56.61°C at using magnetic water with single glass cover [A16]. Dubey et al. conducted a thermo-exergo economic analysis of double slope solar still with $2m^2$ area augmented with ferrite ring magnets and a blackened galvanized iron sheet [A17]. Divagar et al. performed a thermodynamic analysis of a single-slope solar water desalination unit that incorporated graphite plates and ferromagnetic blocks. The study focused on investigating the system's performance under seasonal weather conditions. By presenting a physical model of the solar water desalination unit, Divagar et al. addressed the assumptions and equations governing the exergy analysis. The results obtained indicated a significant reduction in exergy destruction after integrating

ferromagnetic blocks and graphite plates. Moreover, the findings demonstrated an improvement in the convective heat transfer rate during the evaporation process [A18]. Furthermore, Mahdizadeh et al. conducted a study investigating the impact of a magnetic field on enhancing the performance of a conventional solar water desalination unit and solving its equations [A19]. They introduced a model of the solar water desalination unit, including the governing equations, and took into account the boundary conditions and existing assumptions. The researchers performed calculations to analyze the magnetic field and aimed to improve convective heat transfer and enhance the efficiency of the solar water desalination unit through the magnetic field effect using numerical analysis. Dhivagar et al. investigated the performance of a solar water desalination unit using a novel method for enhancing heat transfer, specifically the application of black iron magnetic powder. They conducted their study under varying solar intensities and different salinity levels of water. In this research, 39.8% higher evaporative and 14.5% higher convective heat transfer rates were reported [A20]. Moreover, the phenomenon of ultrasonic in solar water desalination units has garnered significant attention from researchers and scientists. Abed et al. conducted an experimental investigation on an enhanced solar water desalination unit, incorporating a high-frequency ultrasonic evaporator and phase change materials. Their study aimed to explore the effects of ultrasonic on the performance of solar water desalination. A comparison with conventional units led to the conclusion that the use of solar collectors and high-frequency ultrasonic evaporators resulted in a 41.5% increase in water production rate [A21]. Vikram conducted a study on improving heat transfer in solar thermal water desalination. The study centered on the removal of salts with the assistance of ultrasonic. The research involved the examination of materials, experimental methods, and analysis of results to enhance the performance of solar thermal water desalination units through this approach It was deduced from this experiment that the heat transfer rate was found to be higher with a value of 797 W/m^2 K. [A22]. Furthermore, Khoshechin et al. conducted laboratory experiments to investigate the effects of ultrasonic waves on heat transfer enhancement by suspending particles in a fluid to prevent their deposition on the heat transfer surface. The results demonstrated a positive effect on heat transfer, the heat transfer coefficient increased as 8.43% [A23]. Finally, Alwan, N.T. et al. conducted an experimental study on the impact of ultrasonic cold vapor generation on improving the performance of a solar pond desalination unit using fog harvesting technology. They observed an improvement in the evaporative heat transfer coefficient of saline water, as well as increased energy and exergy efficiency, the productivity of the modified solar still increased by 124% [A24]. The existence of a nanofluid that enhances the thermal efficiency of heat transfer systems is considered a fundamental requirement**.** The term "nanofluid" is defined as a dispersion of nanoparticles (typically <100 nm in size) in a base fluid, such as water or ethylene glycol [A25]. It could be defined as a mixture of nanoparticles and conventional liquids [A26]. Despite some limitations such as relatively high preparation costs and stability issues, efforts have been made to develop the nanofluids application in energy systems [A27-32] Ferrofluid, as its name suggests, is a fluid with magnetic properties which placed in a magnetic field, attracted to it, and moves with it [A33]. Fe_3O_4 nanoparticles exhibit magnetic properties, making them attractive materials for the electronic industry and potential future biomedical device applications [A34]. In recent years, magnetic fluids have found numerous applications in the field of heat transfer, attracting significant attention from researchers due to their unique properties [A35]. Among nanoparticles, iron oxide nanoparticles are widely used nanomaterials. Iron oxides have 16 different phases, characterized by a three-dimensional iron lattice structure, low solubility, and distinct colors. Among iron oxides, Fe_3O_4 has received more attention due to its unique properties, including superparamagnetic behavior, low Curie temperature, non-toxicity, and others. This nanofluid possesses an inverse spinel crystal structure, where each unit cell consists of 32 oxygen atoms. The oxygen atoms in the structure of Fe_3O_4 are arranged in a cubic structure with 6-coordinated iron atoms at the corners. In this crystal structure, the Fe (II) ions and half of the Fe (III) ions occupy the octahedral sites while the remaining half of the Fe (III) ions occupy the tetrahedral sites. Iron atoms tend to preferentially occupy octahedral sites due to the higher stability of the crystal field energy, resulting in their dual valency behavior [A6].

Goharkhah investigated forced convection heat transfer using an aqueous-based ferrofluid of Fe_3O_4 under a non-uniform alternating magnetic field. The results, compared using the Reynolds number, indicate an improvement in heat transfer [A36]. Ashjaei et al. investigated the effect of applying a magnetic field on forced convection heat transfer and pressure drop of an aqueous-based nanofluid of Fe_3O_4 in a miniature heat sink. They concluded that heat transfer was enhanced [A37]. In a study conducted by Wang et al., nanofluids consisting of PDA-coated spherical nanoparticles of Fe_3O_4 were used for the first time as photothermal materials, achieving 69.93% evaporation under low irradiance (low light scattering) conditions, with a thermal conductivity of 1 kw/m^2 [A38]. Miaki et al. conducted experiments using Fe_3O_4 – NPs (nanoparticles) due to their unique properties such as superparamagnetic behavior, biocompatibility, biodegradability, and non-toxicity to humans [A39]. Alizadeh jajarm et al. in an experimental work showed that the use of nanofluid reduces the thermal resistance and improves the thermal performance of the device [A40]. This paper includes the results of a research study carried out at Mashhad Azad University for the development of a more efficient solar desalination system. The present work was conducted to improve and increase this device's efficiency and water output by examining magnetic field impact using Fe_3O_4 ferrofluid. Also, the ultrasonic phenomenon's effect to increase the device's efficiency is carried out. In this experimental work, the operation of a cascade solar desalination system under the influence of a magnetic field created by an internal solenoid is conducted. This approach takes into consideration experimental assumptions such as the complete insulation of the desired walls and appropriate water distribution on the cascades, thereby providing improved conditions, including the complete rotation of condensed vapor within the system and achieving complete desalination. The results of this research can be used to increase the efficiency of solar still.

2. Experimental setup

Fig. 1 illustrates the desired solar water desalination device. Step solar desalination is one of the simple distillation desalination devices that are used in the field of water purification. The device casing is constructed from a 0.25-millimeter-thick sheet of galvanized steel. Galvanized steel was chosen for its corrosion resistance and thermal conductivity properties.

This new design included preheating pipes that are placed at the top of the desalination system. These connection pipes which are located between the tank and the device, are shown in Fig. 2. The modified solar still contains 28 steps in three different stepped surfaces built on 2 mm thickness iron sheet. The step dimension is 840 mm*30 mm*110 mm.

The device's stairs have a vital role in facilitating water flow and achieving the necessary temperature for evaporation. By passing through the stairs, water gradually evaporates and condenses on the upper glass surface of the device. The stairs are constructed using galvanized steel and are black stained to enhance the absorption of device stairs' solar radiation. Each step is designed with a gap to allow water to flow downwards to the lower steps.

By creating greenhouse conditions, the glass induces the formation of vapor inside the internal chamber of the device. In this experiment, a 3-millimeter-thick glass with a 15-degree slope is installed on the top surface of the device. This glass not only allows sunlight to pass through but also aids in the condensation of the vapor produced.

By equipping the upper part of the device with glass, a passage is created to collect the condensed water. The 15-degree slope of the glass Facilitates the rapid movement of water droplets towards the pathway, where they are gathered. To ensure water tightness, the mentioned glass is securely sealed using a specialized adhesive. Fig. 3(a) illustrates the upper glass of the device and its corresponding passage.

The water outputs of the device are connected to collection hoses, enabling the transfer of condensed water to the intended container. To transfer water from the tank, which is coated with black color, two sets of black-colored coiled pipes have been employed. The coiled pipes on the right side are connected to the right valve of the tank, while the coiled pipes on the left side are connected to the left valve of the tank. The simultaneous use of two valves connected to the coiled pipes allows for even water distribution onto the stairs. By increasing the output flow rate, a higher level of condensation can be achieved.

Fig. 1: Solar Water Desalination Device.

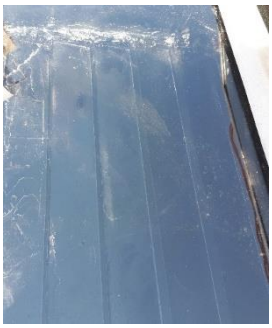

Fig. 2: The lower section of the stairs in the solar still

Fig. 3(b) illustrates the two valves on the right and left sides of the tank and their connection to the preheating pipes. In June and July 2023, the experiments were carried out at 8:00 and lasted until 17:00. At first, salt water was purred into the device. For comparison of a simple solar still to another one with Fe_3O_4 and magnetic field applied by magnetic sheets and solenoids,8 experimental designs on the device were conducted and have been explained in the following.

(a) (b)

Fig. 3: (a) Top glass of the device and the collection passage for condensed water. (b) Right and left valves of the tank and collection passage for condensed water their connection to the device tank.

3. Experimental procedure

In order to prepare nanofluids, Fe3O4 nanoparticles with specifications of 4.8-5.1 g/cm3 specific density and 80 W/m K thermal conductivity were provided by an Iranian nanomaterial company. Fe3O4 characteristics are indicated in Table 1.

Table 1: Physical properties of Fe_3O_4 nanoparticles

Quality	Specifications
Purity	98%
Nanoparticles diameter	20-30 nm
Thermal conductivity	80 W/m. K
True density	4.8-5.1 g/cm^3
Color	Dark Brown
Morphology	spherical

In this research, nanofluid samples with concentration of 0.1% were applied. Samples were exposed to ultrasonic waves through water for duration of 90 minutes. For preparation of magnetic nanofluid a two-step method is followed which is described below:
In accordance with a study by Alizadeh jajarm et al. [A40] sonic exposure and environment pH of 10 and also applying tetra methyl ammonium hydroxide with the 3:1 ratio as surfactant could decrease the impact of agglomeration. The role of surfactants in the nanofluid is decreasing the surface tension which helps to ease separation of droplets from the water surface leading to increase heat transfer coefficient. In order to access homogenous distribution and de-agglomeration of the Fe_3O_4 particles in the water, a 40 kHz ultrasonic waves were produced by an ultrasonic device for duration of 90 minutes. The preparation process is demonstrated in Fig. 4 step by step. A stirrer was applied to mix

Fe_3O_4 nanoparticles with the base fluid. Liquid sonication was performed by the ultrasonic oscillator device for 5 hours. The bath sonicator works with 120V/AC220~240V 50/60 Hz, AC 100 power supply which produces 45 kHz working frequency. The level of sedimentation of the suspension in this study is also shown in Fig. 4. Nanoparticles were easily dispersed in organic thinners. A 0.60 mT (600 Gauss) magnetic field was produced by a 2-A electric current in this experiment.

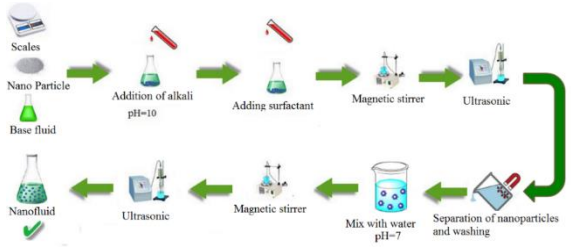

Fig 1. Preparation steps of Fe_3O_4 + water

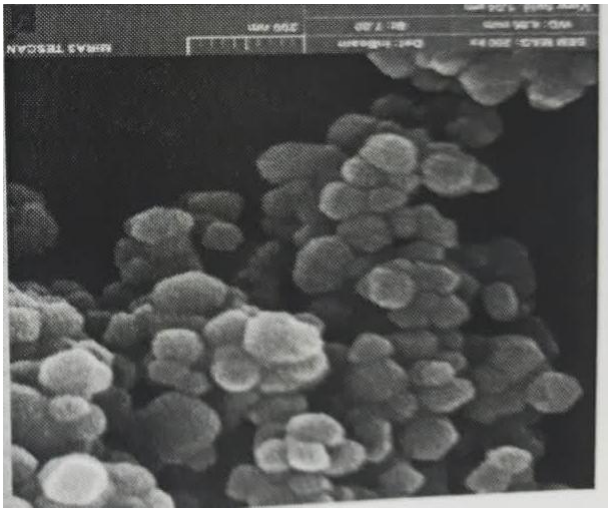

Fig 2. Fe_3O_4 nano particles for composition

Fig. 6 illustrates the settling of Fe_3O_4 +water in immobilized fluid after ultra-sonication and after 15 and 27 days.

Fig 3. (a) Image of synthesized nanofluids immediately after ultra-sonication. (b) Image of synthesized nanofluids after 15 days. (c) Image of synthesized nanofluids after 27 days.

Fig. 7a displays Zeta potential values for Fe_3O_4 nanoparticles. In Fig. 7b the size spectrum of the particles in the nanofluid is showed. This information is obtained using the dynamic light scattering (DLS) method. The average size of Fe_3O_4 + water is approximately 20 nm which is shown in Fig. 8a.

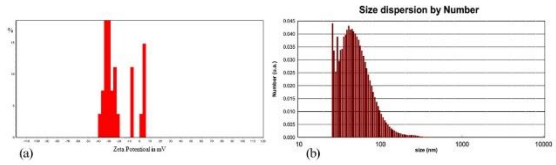

Fig 4. (a) Zeta potential values for Fe_3O_4 nanofluids (b) Nanoparticles size distribution.

As shown in Fig. 8, in reaction to approaching the magnet to the compartment that contains the nanofluid, the nanoparticles moved toward the magnet which confirms the correctness of the prepared nanofluid magnetism.

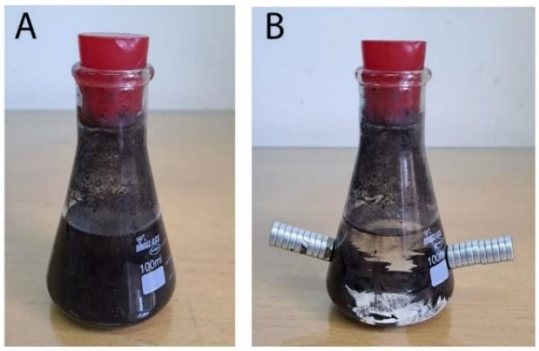

Fig 5. (A) Ferrofluid. (B) Magnetite nanoparticles attracted by magnet

4. Theoretical calculation

The heat transfer in solar still does not last long because of temporary temperature difference in connective parts. Between the inside of glass cover and the water surface is the place that the internal transfer takes place. The convective heat transfer rate is related to water vapor resulted from the effect of thermal radiation between the condensation cover and the water surface. Equation 1. Represents this content. Natural convection happens in the solar still and its direction of flow is represented by the Grashof number. The relationship between Pr, Gr, and Nusselt number is given in Equation 2. In the presence of a magnetic field, when the magnetic field is created by solenoids with 275 and 1000 turns, the magnetic field strength for a solenoid with several turns N could be calculated as Equation 3. In this experiment, the magnetic field is applied with magnetic filling sheets, and two solenoids at different turns of 275 and 1000. μ_0 is the permeability constant, which represents the magnetic permeability.

$$q^{"} = h\Delta T \quad (1)$$

$$Nu = \frac{hl}{k} = C(Gr * Pr)^n \quad (2)$$

$$B = NI\mu_\circ \quad (3)$$

Where,

$$\mu_\circ = 4\pi * 10^{-7} \quad (4)$$

In the results section, the variations of the Nusselt number and the Grashof number with respect to the magnetic field strength generated by different solenoids and a constant magnetic field have been investigated, according to the Hartmann number. For the mentioned calculations, Equations 5-8 have been used. Ra represents the dimensionless Rayleigh number, and Gr represents the dimensionless Grashof number.

$$Ra = \frac{g\beta\Delta TL^3}{\vartheta\alpha} \quad (5)$$

$$Ra = Gr\ Pr \quad (6)$$

$$Nu = 0.68 + \frac{0.67Ra^{0.25}}{\left[1 + \left(\frac{0.492}{pr}\right)^{\frac{9}{16}}\right]^{\frac{4}{9}}} \quad (7)$$

$$Gr = \frac{g\beta(T_s - T)}{v^2}L^3 \quad (8)$$

The solar still efficiency could be defined as below:

$$\eta = \frac{V_F^T \rho h_{fg}}{H} \quad (9)$$

Where,

$$h_{fg} = 2450 \quad \frac{KJ}{Kg} \quad (10)$$

$$H = A_s * \int I_T(t)dt = A_s * \sum_i I_T(t_i)\Delta T$$

5. Experimental results

The experiments were conducted under various conditions, including 1) Simple condition 2) In conjunction with magnetic sheets 3) In conjunction with two solenoids with 275 and 1000 turns 4) In conjunction with Fe_3O_4 nanofluid 5) In conjunction with Fe_3O_4 nanofluid and magnetic sheets 6) In conjunction with Fe_3O_4 nanofluid with solenoids of 275 and 1000 turns 7) In conjunction with the phenomenon of ultrasonic 8) In conjunction with Fe_3O_4 nanofluid, solenoid, and optimized ultrasonic phenomenon. These experiments were performed, analyzed, and optimized. They were conducted during sunny days, specifically from June 28th to August 2nd, 2023. The experiments were carried out between 9 AM to 3 PM, and the detailed reports were documented on an hourly basis. Additionally, the experiments were repeated on two different days to ensure reliable and consistent results.

The magnet field significantly reduces the surface tension of salty water, which leads to increased evaporation. Therefore, the application of magnetic field using solenoid has been investigated in this experiment. Linear solenoids are essentially composed of a coiled electric wire wound around a cylindrical tube and a ferromagnetic plunger. The wire coil is located inside the cylindrical tube, while the ferromagnetic plunger moves inward and outward within the coil body. As seen in Fig. 9(a), for the construction of the solenoid, wire coils with 275 and 1000 turns were used. Inside these wire coils, an iron core is placed. Once connected to a suitable power supply, as depicted in Fig. 9(b), and linked to the mains electricity, the solenoid is prepared for experiments. To prevent the risk of electric shock and burning, cable adhesive has been used for the solenoids, as shown in Fig. 9(c). It was poured into the solenoid container and then placed within the stages of the solar water desalination device.

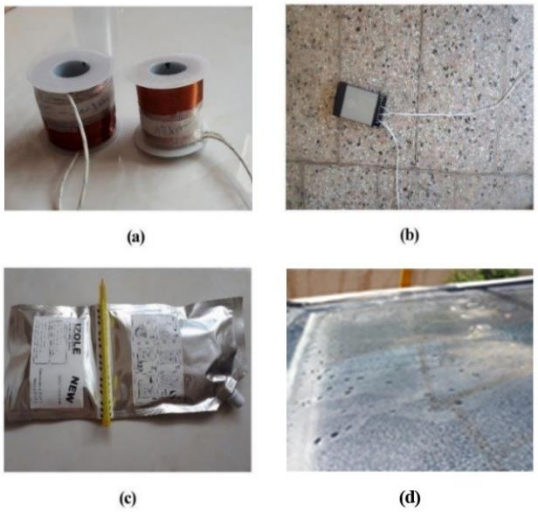

Fig 6. (a) Preparation of solenoids with 275 and 1000 turns using wire coils. (b) Power supply for the solenoids. (c) Cable adhesive. (d) Condensation on the Css glass.

Fig. 10 corresponds to the first experiment conducted on June 28th, 2023. The experiment took place on a

clear and sunny day using a conventional solar water desalination device. It should be noted that the experiments were conducted over two consecutive days, and the reported data in this article represents the maximum values obtained during these experiments. The water temperature touched approximately $56^{\circ}C$, this is caused by the absorptive capacity of the radiation heat pipes.

Fig. 11 represents the result of the second experiment, which involved conducting tests with fixed magnetic sheets. The experiment was performed on June 30th and July 2nd, 2023, using a solar water desalination device. It is important to note that the reported data represents the maximum possible values from these experiments.

Fig. 12 illustrates the results of the experiments conducted using a solar water desalination device with a solenoid having 275 turns on two dates, July 7th and 8th, 2023. Please note that only the maximum values obtained from these experiments have been reported.

Fig. 13 depicts the results of the experiments conducted using a solar water desalination device with a solenoid having 1000 turns on two days, July 9th and 10th, 2023. It is important to note that only the maximum values obtained from the experiments have been reported in this section.

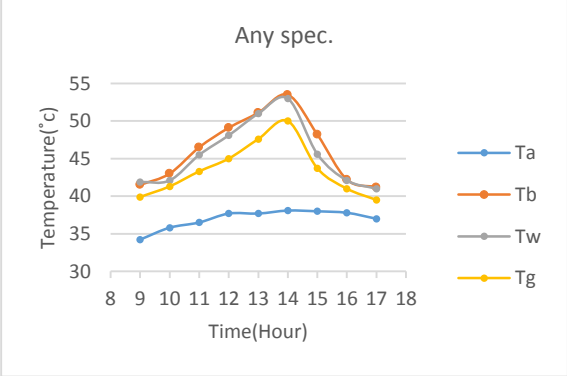

Fig 7. Temperature of air, glass coating, water, and heat transfer coefficient in Design 1

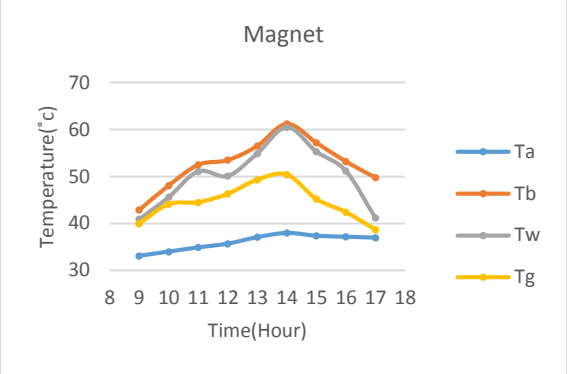

Fig 8. Temperature of air, glass coating, water, and heat transfer coefficient in Design 2.

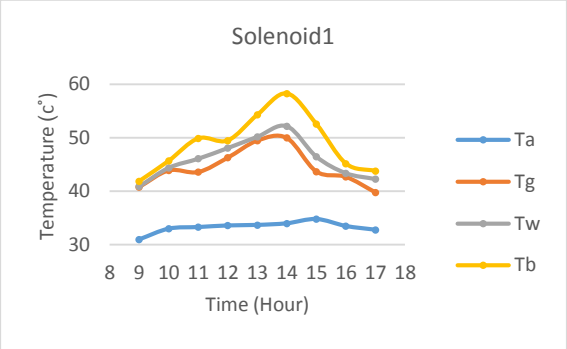

Fig 9. Temperature of air, glass cover, water, and heat transfer coefficient in design 3

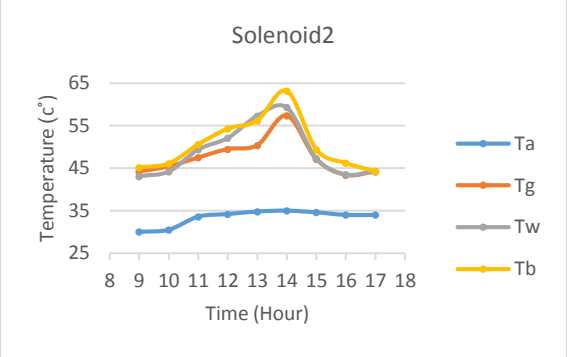

Fig 10. Temperature of air, glass cover, water, and heat transfer coefficient in design 4

Fig. 14 corresponds to the experiment conducted on a solar water desalination device with the injection of Fe_3O_4 solution on two consecutive days, July 13th and 14th, 2023. In sections 2-6 of the article, a detailed explanation of the nanoparticle preparation method has been provided. Based on the volume of the water tank, a quantity of 25 milliliters of nanoparticle solution was injected into the tank. The temperatures mentioned in the chart represent the maximum values obtained during the experiments on the specified days.

Fig. 15 investigates the combined effect of

nanoparticle with the magnetic sheets installed in the lower section of the staircase in the corresponding chamber. The experiment was conducted on July 15th and 16th, 2023 under clear and sunny weather conditions. However, the maximum possible value was reported on July 15th, 2023.

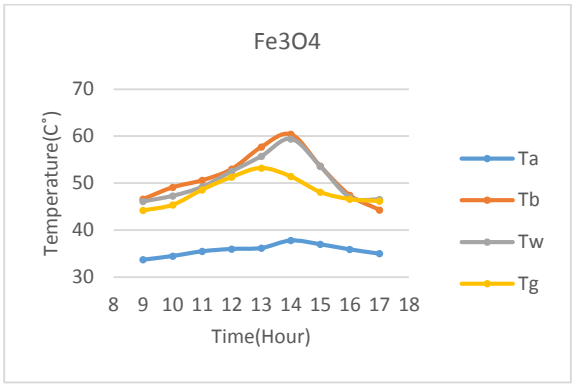

Fig 11. Temperature of air, glass cover, water, and heat transfer coefficient in design 5

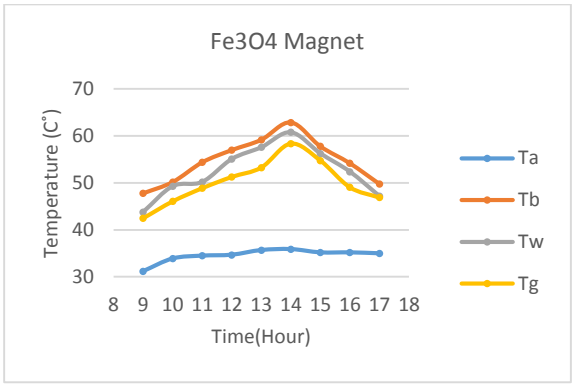

Fig 12. Temperature of air, glass cover, water, and heat transfer coefficient in design6

Experiments were carried out on the solar water desalination device with the injection of nanoparticle solution in the presence of a magnetic field applied using a solenoid with 1000 turns on clear and sunny days, July 19th and 20th, 2023. Similarly, a solenoid with 275 turns, connected to the power supply and city electricity at its two ends, was placed in the staircase section of the solar water desalination device. To ensure safety in the presence of humid air inside the device, the solenoid was properly sealed to prevent electric shock hazards.

Together with the nanoparticle material, experiments were conducted on July 22nd and 23rd, 2023. It should be noted that in Fig. 17, the best results for the temperature of air, glass coating, water, and heat transfer coefficient are presented.

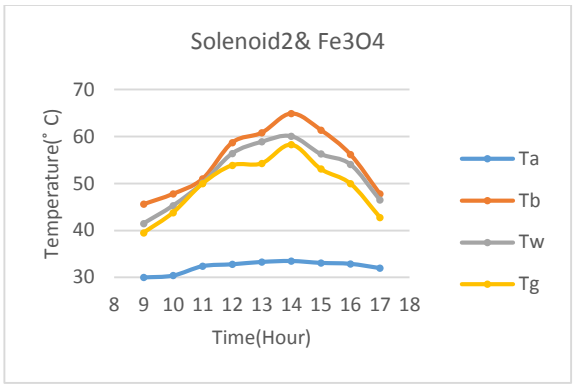

Fig 13. Temperature of air, glass cover, water, and heat transfer coefficient in plan 7

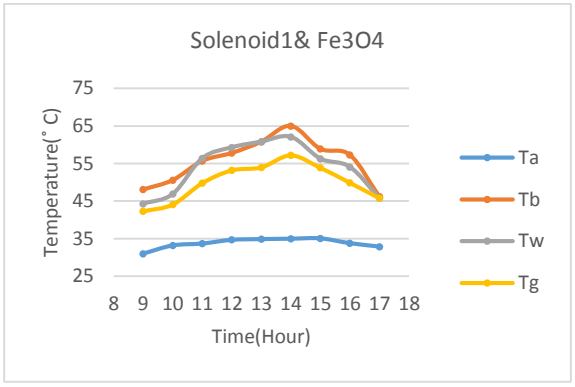

Fig 14. Temperature of air, glass cover, water, and heat transfer coefficient in plan 8

The term ultrasound refers to sound waves with a frequency higher than the highest range of human hearing, which is approximately 16-20 kHz [A41]. One of the methods used in modern oxidation processes for water and wastewater treatment is ultrasonic irradiation [A42]. therefore, In the experiment, for increasing the rate of heat and mass transfer, the water in the desalination device's tank was repeatedly subjected to ultrasonic waves using a Paxson ultrasonic cleaner model with specifications of 50 W, 220 V, and 50 Hz. After preparation, the water was poured into the solar water desalination device. The experiments took place on July 25th and 26th, 2023, under sunny and clear weather conditions. The best result was reported on July 25th, 2023 and the corresponding graphs can be found in Fig. 18. In the latest experiment, which was the primary focus of the research, all factors, including the presence of a magnetic field applied with the solenoid, and the application of nanoparticle fluid on ultrasonic water, were tested simultaneously. An important point to consider is the variations in air temperature over a relatively long period during the experiments had

some influence on the results. The experiments with all the mentioned factors on the rate of water production in the solar water desalination device were conducted on August 2nd and 3rd, 2023. The results of the best-case scenario can be found in Fig. 19. comparing with design1 in this mode the basin temperature has reached the highest value of 66.8˚c at 2 PM. experimental results indicate that as the intensity of the magnetic field increases, more heat is transferred to the water, leading to an enhanced rate of desalinated water production.in other word the larger the coil turns of solenoid , the stronger the magnetic field and leads to an enhanced rate of desalinated water production.

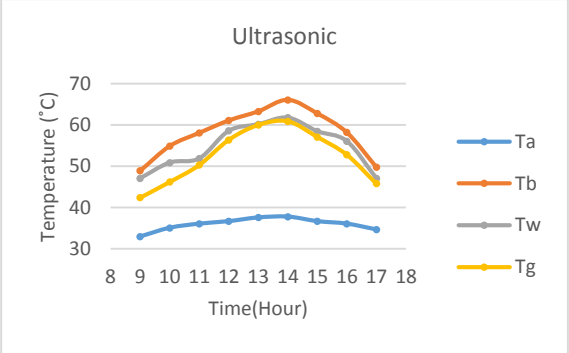

Fig 15. Temperature of air, glass cover, water, and heat transfer coefficient in design 9

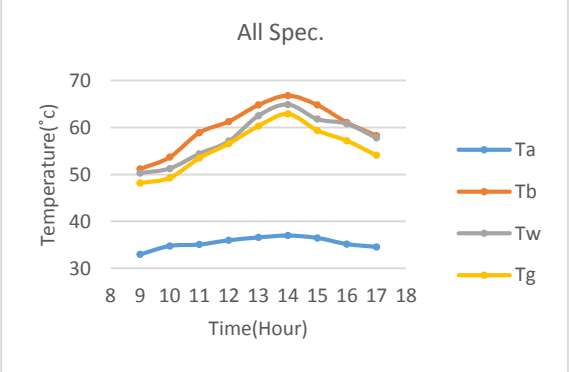

Fig 16. Temperature of air, glass cover, water, and heat transfer coefficient in design 10

It is worth noting that the primary reason for freshwater production in solar water desalination devices is the temperature difference between the water inside the heat exchanger and the glass.

Fig. 20 and 21 depict the temperature profiles of the water in the heat transfer coefficient and the glass coating, respectively. By comparing these graphs, it can be concluded that Design 10, which utilizes ultrasonic water, will yield the highest efficiency in the solar water desalination device. Furthermore, in Design 8, the significant temperature difference is due to the presence of a solenoid with 1000 turns and the utilization of nanofluid, which results in the magnetization of the present nanofluid.

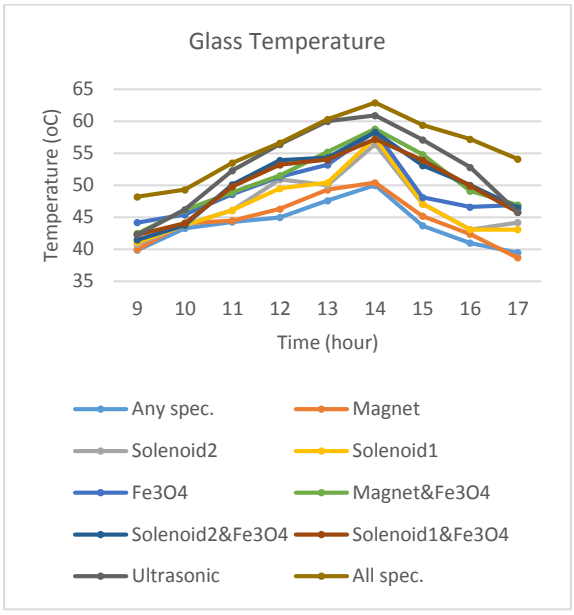

Fig 17. The average temperature of the glass coating over time in 10 designs

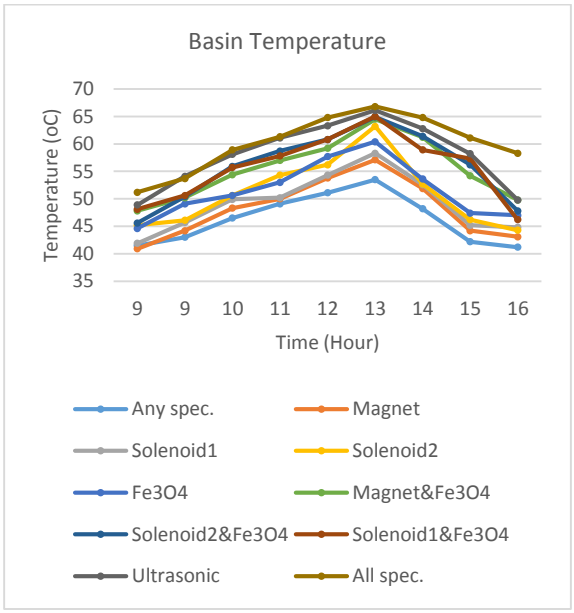

Fig 18. The average water temperature of the heat transfer coefficient in relation to time in 10 plans

The relationship between the production rate at each stage of the experiment per hour is depicted in Fig. 22. As evident from the graphs, Design 10 exhibits the highest water production rate among the tested

designs. Compared to Design 1, which represents a simple stepped solar water desalination device, the water production rate has increased in Design 10. The efficiency of the solar desalination device in design10 compared to design1 with an efficiency of 31.8% has reached to 50.51%.

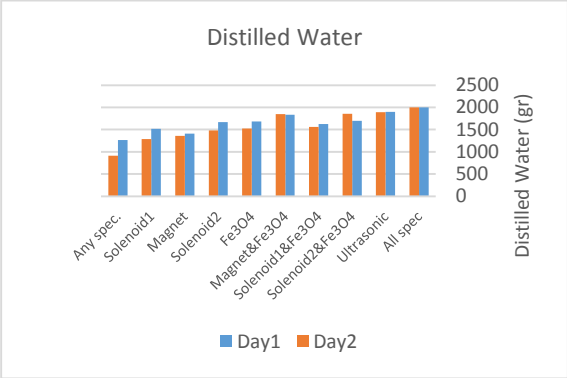

Fig 19. represents the daily water production rate for the 10 experimental designs

As described in the governing equations section, by using the provided calculations and computing the heat transfer, we have generated the temperature variation profiles for three designs: a constant magnetic field with magnetic plates, which applies 0.11T magnetic field magnitude, a solenoid with 275 turns, and a solenoid with 1000 turns, which apply 0.314T and 1.256T magnetic field magnitudes. These profiles are depicted in Fig. 23.

Based on the graph, it is evident that the design associated with the solenoid with 1000 turns experiences the highest Hartmann number, and the Nusselt number reaches its highest value among the three designs. Following that, the solenoid with 275 turns exhibits the next highest Nusselt number, and ultimately, the design with fixed iron plates is observed.

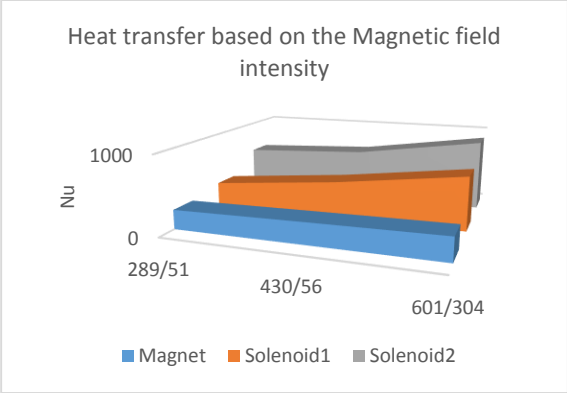

Fig 20. represents the graph of the heat transfer ratio as a function of magnetic field intensity

6. Economic and Uncertainty Analysis

Uncertainty assessment helps to understand the errors in the evaluated quantities from the measured ones [A43]. Different variables in measurements like calibration, recording, monitoring, etc. lead to uncertainty. Variables like Ambient air temperatures, air velocity and sun radiation are considered for calculating in the experiments. Different reasons can occur for experimental errors and they could be of different origins and nature, random errors, fixed errors, etc. Experiment errors, can the result in uncertainty in D_R. B_i (i=1 to n) are uncertainties in the independent variable and D is the dependent variable, where X (i=1 to n) is the independent variable. Therefore, uncertainty is given by Eq. (11). [A44]

$$D_R = \left(\frac{\partial D}{\partial X_1} B_1\right)^2 + \left(\frac{\partial D}{\partial X_2} B_2\right)^2 + \left(\frac{\partial D}{\partial X_3} B_3\right)^2 + \cdots \left(\frac{\partial D}{\partial X_n} B_n\right)^2 \quad (11)$$

According to the basic parameters of the experiment, the formula can be expanded to check the uncertainty analysis in solar stills, too. Table 2 provides the precision levels of the devices used in these experiments, contributing to obtaining more accurate results.

Table 2: The accuracy of test equipment

Device name	Domain	Accuracy of the device
Solarimeter	0-200000 lux	-3-+3
Laser thermometer	-50 -400 ℃	-1.5-+1.5
Erlen	0-50 ml	-5 ml-+5ml

7. Conclusion

The experimental section and the obtained results demonstrate that the utilization of ultrasonic-assisted water treatment in the presence of a magnetic field generated by a solenoid with 1000 turns and the use of nanofluid significantly increases the daily production rate of desalinated water and enhances the device's efficiency. Several factors contribute to this increase in water production rate. The following are some possible factors:

- The use of Fe_3O_4 nanofluid or magnetite, which is the most magnetic material on the planet, leads to an augmentation in the rate of water production. In this case, the solar still efficiency is estimated about 73.7%.
- The use of magnetic field, which is applied by a magnet or solenoid, leads to an improvement in the

solar still efficiency compared to mode1.When magnetic field is applied by a magnet or a solenoid with 1000 and 275 turns, the solar still efficiency respectively, is estimated about 64.3%,72.9% and 66.3%.

- The application of a magnetic field on the Fe_3O_4 nanofluid, which exhibits a strong response to magnetic fields, results in a higher water production rate compared to the initial state of the device. The previous section's results indicate that as the intensity of the magnetic field increases, more heat is transferred to the water, leading to an enhanced rate of desalinated water production. When the magnetic field is applied by a magnet or a solenoid with 1000 and 275 turns on the Fe_3O_4 nanofluid, the solar still efficiency respectively, is estimated at 80.2%,74.3%, and 70.1%.
- The use of sonicated water, has led to a higher production of desalinated water compared to mode 1and the temperature difference of glass and basin in the result section confirms this issue. In this case, the solar still efficiency is estimated at 83.1%.
- The usage of sonicated water in the presence of a magnetic field and iron oxide (Fe_3O_4), which possesses the highest magnetic properties and exhibits a strong response to magnetic fields, has led to a higher production of desalinated water compared to the simple design of the solar desalination device (referred to as Design 1) used in the study. In this case, the solar still efficiency is estimated about 87.5%.

Nomenclature

A	Cross-section (m^2)
A_s	Glass Cross-section (m^2)
B	Magnetic field intensity (T)
g	Gravity ($^N/_{Kg}$)
Gr	Dimensionless Grashof number
h	coefficient of heat transfer (W m^{-2} K^{-1})
I	Electric current (A)
I_t	Solar radiation intensity (Kwhm^{-2})
L	Characteristic length (m)
N	Number of coil turns
Nu	Dimensionless Nusselt number
Pr	Dimensionless Prandtl number
q"	heating power (Wm^{-2})
R	Electrical resistance (Ω)
Ra	Dimensionless Rayleigh number
T	Temperature (^oC)
V_T^F	Hourly amount of water produced (Kgh^{-1})

Greek symbols

α	Thermal Diffusivity (m^2s^{-1})
β	Thermal Expansion (K^{-1})
Δ	Uncertainty (-)
ρ	density (kg m^{-3})
μ	dynamic viscosity (kg m^{-1} s^{-1})
μ_0	Vacuum Permeability (Hm^{-1})
υ	Cinematic Viscosity (m^2s^{-1})
σ	Electrical Conductivity (Nm^{-2})

Subscripts

S	Surface
∞	Environment

References

[A1] Mandev, E., Muratçobanoğlu, B., Manay, E., & Şahin, B. (2024). Desalination performance evaluation of a solar still enhanced by thermoelectric modules. Solar Energy, 268, 112325. https://doi.org/10.1016/j.solener.2024.112325

[A2] Toosi, S. S. A., Goshayeshi, H. R., Zahmatkesh, I., & Nejati, V. (2023). Experimental assessment of new designed stepped solar still with Fe_3O_4+ graphene oxide+ paraffin as nanofluid under constant magnetic field. Journal of Energy Storage, 62, 106795. http://dx.doi.org/10.1016/j.est.2023.106795

[A3] Assari, M. R., Esfandeh, E., & Baharvand, R. (2022). Experimental investigation of effect of using sand on the performance of solar still. Journal of Renewable and New Energy, 9(1), 87-93. https://dorl.net/dor/20.1001.1.24234931.1401.9.1.9.0

[A4] Abdullah, A., Essa, F. A., Panchal, H., Alawee, W. H., & Elsheikh, A. H. (2023). Enhancing the performance of tubular solar stills for water purification: a comprehensive review and comparative analysis of methodologies and materials. Results in Engineering, 101722. https://doi.org/10.1016/j.rineng.2023.101722

[A5] Toosi, S. S. A., Goshayeshi, H. R., & Heris, S. Z. (2021). Experimental investigation of stepped solar still with phase change material and external condenser. Journal of Energy Storage, 40, 102681. https://doi.org/10.1016/j.est.2021.102681

[A6] Goshayeshi, H. R., & Safaei, M. R. (2020). Effect of absorber plate surface shape and glass cover inclination angle on the performance of a passive solar still. International Journal of Numerical Methods for

Heat & Fluid Flow, 30(6), 3183-3198. https://doi.org/10.1108/HFF-01-2019-0018

[A7] Mohammad Reza, S., Hamid Reza, G., & Chaer, I. (2019). Solar still efficiency enhancement by using graphene oxide/paraffin composite. Energies, 12(10), 2002. https://doi.org/10.3390/en12102002

[A8] Abdelamir, H. S., Hachim, D. M., & Al-Shamani, A. N. (2024). Review study the maximum productivity of all types of solar still with and without modification. AIP Conference Proceedings. https://doi.org/10.1063/5.0191752

[A9] Chauhan, R., Dumka, P., & Mishra, D. R. (2022). Experimental evaluation and development of artificial neural network model for the solar stills augmented with the permanent magnet and sandbag. Journal of Advanced Thermal Science Research, 9, 9-23. https://doi.org/10.15377/2409-5826.2022.09.2

[A10] Abdel-Aziz, E. A., Mansour, T. M., Dawood, M. M. K., Ismail, T. M., & Ramzy, K. (2023). Exergoeconomic and enviroeconomic evaluations of conventional solar still using PCM and electric heater powered by solar energy: an experimental study. Environmental Science and Pollution Research, 30(24), 66135-66156. https://doi.org/10.1007/s11356-023-26761-4

[A11] Goshayeshi, H. R., Chaer, I., Yebiyo, M., & Öztop, H. F. (2022). Experimental investigation on semicircular, triangular and rectangular shaped absorber of solar still with nano-based PCM. Journal of Thermal Analysis and Calorimetry, 1-13. https://doi.org/10.1007/s10973-021-10728-z

[A12] Alawee, W. H., A Hammoodi, K., Dhahad, H. A., Omara, Z., Essa, F. A., Abdullah, A., & Amro, M. I. (2023). Effects of magnetic field on the performance of solar distillers: a review study. Engineering and Technology Journal, 41(1), 121-131. https://doi.org/10.30684/etj.2022.134576.1240

[A13] Wu, S., & Zhang, F. (2006). Effects of magnetic field on evaporation of distilled water. Abstracts of papers of the American Chemical Society (Vol. 232, pp. 954-954). 1155 16TH ST, NW, Washington, DC 20036 USA: Amer Chemical Soc.

[A14] Amor, H. B., Elaoud, A., Salah, N. B., & Elmoueddeb, K. (2017). Effect of magnetic treatment on surface tension and water evaporation. Int. J. Adv. Ind. Eng, 5, 119-124. http://Dx.Doi.Org/10.14741/Ijae/5.3.4

[A15] Goharkhah, M., & Ashjaee, M. (2014). Effect of an alternating nonuniform magnetic field on ferrofluid flow and heat transfer in a channel. Journal of magnetism and magnetic materials, 362, 80-89. https://doi.org/10.1016/j.jmmm.2014.03.025

[A16] Al-Hilphy, A. R. S. (2013). Development of Basin Solar Stillby Adding Magnetic Treatment Unit and Double Glass Cover Provided with Water. American Journal of Engineering and Applied Sciences, 6(3), 286-296. http://dx.doi.org/10.3844/ajeassp.2013.286.296

[A17] Dubey, M., & Mishra, D. R. (2020). Thermo-exergo-economic analysis of double slope solar still augmented with ferrite ring magnets and GI sheet. Desalination and Water Treatment, 198, 19-30. http://dx.doi.org/10.5004/dwt.2020.25947

[A18] Dhivagar, R., Mohanraj, M., Raj, P., & Gopidesi, R. K. (2021). Thermodynamic analysis of single slope solar still using graphite plates and block magnets at seasonal climatic conditions. Water Science and Technology, 84(10-11), 2635-2651. https://doi.org/10.2166/wst.2021.156

[A19] Mehdizadeh Youshanlouei, M., Yekani Motlagh, S., & Soltanipour, H. (2021). The effect of magnetic field on the performance improvement of a conventional solar still: a numerical study. Environmental Science and Pollution Research, 28, 31778-31791. https://doi.org/10.1007/s11356-021-12947-1

[A20] Dhivagar, R., Shoeibi, S., Kargarsharifabad, H., Ahmadi, M. H., & Sharifpur, M. (2022). Performance enhancement of a solar still using magnetic powder as an energy storage medium- exergy and environmental analysis. Energy Science & Engineering, 10(8), 3154-3166. https://doi.org/10.1002/ese3.1210

[A21] Abed, A. H., Hoshi, H. A., & Jabal, M. H. (2021). Experimental investigation of modified solar still coupled with high-frequency ultrasonic vaporizer and phase change material capsules. Case Studies in Thermal Engineering, 28, 101531. https://doi.org/10.1016/j.csite.2021.101531

[A22] Banakar, V. V., Sabnis, S. S., Gogate, P. R., & Raha, A. (2020). Improvements in heat transfer in thermal desalination operation based on removal of salts using ultrasound pretreatment. Ultrasonics Sonochemistry, 69, 105251. https://doi.org/10.1016/j.ultsonch.2020.105251

[A23] Khooshehchin, M., Ghotbinasab, S., & Mohammadidoust, A. (2021). Experimental study of the effects of ultrasonic waves on surface sediments in pool boiling. Modares Mechanical Engineering, 21(5), 315-326. http://dorl.net/dor/20.1001.1.10275940.1400.21.5.1.7.

[A24] Alwan, N. T., Ahmed, A. S., Majeed, M. H., Shcheklein, S. E., Yaqoob, S. J., Nayyar, A., Nam, Y., & Abouhawwash, M. (2022). Enhancement of the Evaporation and Condensation Processes of a Solar

Still with an Ultrasound Cotton Tent and a Thermoelectric Cooling Chamber. Electronics, 11(2), 284. http://dx.doi.org/10.3390/electronics11020284

[A25] Abd Elbar, A. R., & Hassan, H. (2020). An experimental work on the performance of new integration of photovoltaic panel with solar still in semi-arid climate conditions. Renewable Energy, 146, 1429-1443. https://doi.org/10.1016/j.renene.2019.07.069

[A26] Mahian, O., Kianifar, A., Heris, S. Z., Wen, D., Sahin, A. Z., & Wongwises, S. (2017). Nanofluids effects on the evaporation rate in a solar still equipped with a heat exchanger. Nano energy, 36, 134-155. https://doi.org/10.1016/j.nanoen.2017.04.025

[A27] Navas, J., Sánchez-Coronilla, A., Martín, E. I., Teruel, M., Gallardo, J. J., Aguilar, T., Gómez-Villarejo, R., Alcántara, R., Fernández-Lorenzo, C., & Piñero, J. C. (2016). On the enhancement of heat transfer fluid for concentrating solar power using Cu and Ni nanofluids: An experimental and molecular dynamics study. Nano energy, 27, 213-224. https://doi.org/10.1016/j.nanoen.2016.07.004

[A28] Ni, G., Miljkovic, N., Ghasemi, H., Huang, X., Boriskina, S. V., Lin, C.-T., Wang, J., Xu, Y., Rahman, M. M., & Zhang, T. (2015). Volumetric solar heating of nanofluids for direct vapor generation. Nano energy, 17, 290-301. https://doi.org/10.1016/j.nanoen.2015.08.021

[A29] Jin, H., Lin, G., Bai, L., Zeiny, A., & Wen, D. (2016). Steam generation in a nanoparticle-based solar receiver. Nano energy, 28, 397-406. https://doi.org/10.1016/j.nanoen.2016.08.011

[A30] Milanese, M., Colangelo, G., Iacobazzi, F., & de Risi, A. (2017). Modeling of double-loop fluidized bed solar reactor for efficient thermochemical fuel production. Solar Energy Materials and Solar Cells, 160, 174-181. https://doi.org/10.1016/j.solmat.2016.10.028

[A31] Mahian, O., Kianifar, A., Kalogirou, S. A., Pop, I., & Wongwises, S. (2013). A review of the applications of nanofluids in solar energy. International Journal of Heat and Mass Transfer, 57(2), 582-594. http://dx.doi.org/10.1016/j.ijheatmasstransfer.2012.10.037

[A32] Mahian, O., Kianifar, A., Sahin, A. Z., & Wongwises, S. (2014). Entropy generation during Al2O3/water nanofluid flow in a solar collector: Effects of tube roughness, nanoparticle size, and different thermophysical models. International Journal of Heat and Mass Transfer, 78, 64-75. http://dx.doi.org/10.1016/j.ijheatmasstransfer.2014.06.051

[A33] Durrani, Hosseini, Sardashti, & Shahraki. (2021). Investigating the effect of salt water depth in stepped solar desalination using Comsol software. Journal of separation science and engineering, 12(2), 58-70. https://doi.org/10.22103/jsse.2021.2770

[A34] Lathiya, P., & Wang, J. (2022). Magnetite Nanoparticles ($Fe_3\ O_4$) for Radio-Frequency and Microwave Applications. Iron Oxide Nanoparticles [Working Title]; Intech Open: Rijeka, Croatia. https://doi.org/10.5772/intechopen.104930

[A35] Fadaei, F., Shahrokhi, M., Dehkordi, A. M., & Abbasi, Z. (2017). Heat transfer enhancement of Fe_3O_4 ferrofluids in the presence of magnetic field. Journal of magnetism and magnetic materials, 429, 314-323. https://doi.org/10.1016/j.jmmm.2017.01.046

[A36] Bezaatpour, M., & Goharkhah, M. (2019). Effect of magnetic field on the hydrodynamic and heat transfer of magnetite ferrofluid flow in a porous fin heat sink. Journal of magnetism and magnetic materials, 476, 506-515. https://doi.org/10.1016/j.jmmm.2019.01.028

[A37] Ashjaee, M., Goharkhah, M., Khadem, L. A., & Ahmadi, R. (2015). Effect of magnetic field on the forced convection heat transfer and pressure drop of a magnetic nanofluid in a miniature heat sink. Heat and Mass Transfer, 51, 953-964. http://dx.doi.org/10.1007%2Fs00231-014-1467-1

[A38] Wang, Q., Qin, Y., Jia, F., Song, S., & Li, Y. (2022). Recyclable Fe_3O_4@ Polydopamine (PDA) nanofluids for highly efficient solar evaporation. Green Energy & Environment, 7(1), 35-42. http://dx.doi.org/10.1016/j.gee.2020.07.020

[A39] Yew, Y. P., Shameli, K., Miyake, M., Kuwano, N., Bt Ahmad Khairudin, N. B., Bt Mohamad, S. E., & Lee, K. X. (2016). Green synthesis of magnetite (Fe_3O_4) nanoparticles using seaweed (Kappaphycus alvarezii) extract. Nanoscale research letters, 11(1), 1-7. https://doi.org/10.1186/s11671-016-1498-2

[A40] Jajarm, A. R. A., Goshayeshi, H. R., Bashirnezhad, K., Chaer, I., Toghraie, D., & Salahshour, S. (2024). Combined effect of the magnetic field, orientation, and filling ratio on cylindrical pulsating heat pipe using distilled water and distilled water/Fe_3O_4 nanofluid. Journal of magnetism and magnetic materials, 590, 171712. https://doi.org/10.1016/j.jmmm.2024.171712

[A41] M. Legay, N. Gondrexon, S. Le Person, P. Boldo, and A. Bontemps, "Enhancement of heat transfer by ultrasound: review and recent advances," International Journal of Chemical Engineering, vol. 2011, 2011. https://doi.org/10.1155/2011/670108

[A42] N. Mat Budari, M. F. Ali, K. H. Ku Hamid, and M. Musa, "Ultrasonic Irradiation on Microorganism Disruption in Water Disinfection Process–A Mini Overview," Applied Mechanics and Materials, vol. 754, pp. 676-681, 2015. https://doi.org/10.4028/www.scientific.net%2FAMM.754-755.676

[A43] Devi, M., Dutta, P. P., & Mohanta, D. (2015). Analytical calculation of chain length in ferrofluids. Bulletin of Materials Science, 38, 221-226. https://doi.org/10.1007/s12034-014-0812-9

[A44] Dutta, P., Dutta, P. P., Kalita, P., Goswami, P., & Choudhury, P. K. (2021). Energy analysis of a mixed-mode corrugated aluminum alloy (AlMn1Cu) plate solar air heater. Materials Today: Proceedings, 47, 3352-3357. https://doi.org/10.1016/j.matpr.2021.07.156